Isogeometric analysis of plane curved beams

Antonio Cazzani[a], Marcello Malagù[a], Emilio Turco[b]

[a]*Dipartimento di Ingegneria Civile, Ambientale e Architettura (DICAAR), Università degli Studi di Cagliari, Italia*
[b]*Dipartimento di Architettura, Design e Urbanistica (DADU), Università degli Studi di Sassari, Italia*

Abstract

A curved beam element based on Timoshenko model and NURBS (Non-Uniform Rational B-Splines) interpolation both for geometry and displacements is presented. Such element can be used to suitably analyze plane curved beams and arches. Some numerical results will explore the effectiveness and accuracy of this novel method by comparing its performances with those of some accurate finite elements proposed in the technical literature and also with analytical solutions: for those cases where such closed form solutions were not available in the literature, they have been computed by exact integration of the governing differential equations. It is shown that the presented element is almost insensitive to both membrane- and shear-locking, and that such phenomena can be easily controlled by properly choosing the number of elements or the NURBS degree.

Keywords: NURBS, Isogeometric analysis, curved Timoshenko beam.

1. Introduction

Finite element models usually do not replicate the exact geometry of a solid defined by a Computer Aided Design (CAD) representation: the finite element mesh is only an approximation of the exact CAD geometry, so the precision of the finite element (FE) analysis can be affected by errors originating from geometric description. Isogeometric analysis, whose name was coined by Hughes [1], attempts to avoid this problem, by integrating the geometry model defined by CAD into the FE analysis in order to solve the underlying problem without any shape approximation.

In the last years, many efforts in the framework of isogeometric analysis have been done (see e.g. [2] and [3]) and there are interesting results for a

wide range of problems such as vibrations and wave propagations, nearly incompressible solids, fluids, fluid-structure interaction. The geometric settings, however, mostly concern 2-D and 3-D continuum models or shell-like structures [4].

It appears that, up to the last two years, special structural elements for 1-D problems based on the isogeometric concept were still lacking, even if the use of B-spline had been reported, for instance, in [5], [6] and [7]. Recently, however, a strong interest for such elements has been developing, and several contributions appeared: see, for instance [8], [9], [10], [11], [12], [13], [14], [15]. In these papers both straight and spatial Timoshenko beams have been considered, with particular emphasis on locking control.

Here, a plane curved Timoshenko beam element based on NURBS interpolation for both geometry and displacements, which is able to analyze plane arches and beams, has been developed. In Section 2 we discuss the basic key points of the mechanical model besides to the guidelines of the NURBS interpolation giving all the details useful to implement the numerical model. Successively, in Section 3, various numerical results are presented with the goal to explore the effectiveness and accuracy of this novel method by comparing its performances with those of finite elements already available in the technical literature and with analytical solutions. In particular, some exact solutions, which were not yet available in the literature, have been computed in order to test the numerical solutions and verify the reference values used by other authors for comparing their results. Finally, in Section 4, some concluding remarks and future developments are briefly reported.

2. NURBS representation of plane curved Timoshenko beams

We consider a curved plane beam (see Figure 1) whose centroid line is a plane curved parametrized by the arc-length $s \in [0; \ell]$. We suppose also that one of the principal inertia axis and the shear center of the cross-section lie in the same plane. Let the global reference system be denoted by $(O; x_1, x_2)$ and the local one by $(o; t, r)$, t and r being respectively the tangent and the normal unit vectors to the curve. Moreover, we denote by R the curvature radius and by $(\cdot)'$ the derivatives with respect to the arc-length s. With this notation, the differential form of equilibrium and kinematic compatibility equations and the constitutive law describing the curved Timoshenko plane

Please cite this document as: A. Cazzani, M. Malagú, and E. Turco "Isogeometric analysis of plane–curved beams" *Mathematics and Mechanics of Solids*, 2016, 21(5): 562–577 DOI:10.1177/1081286514531265

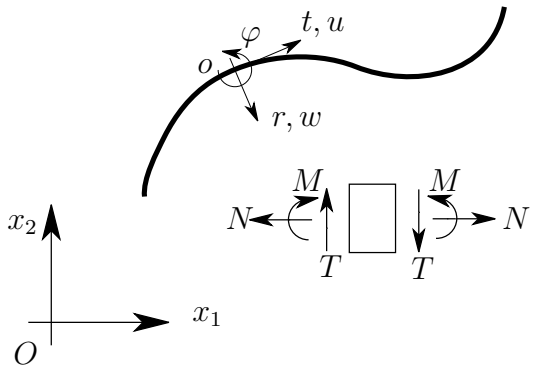

Figure 1: Plane curved beam: centroid line and reference systems.

beam problem in the local reference system are:

$$N' - \frac{T}{R} + q_t = 0, \qquad T' + \frac{N}{R} + q_r = 0, \qquad M' - T + m = 0, \tag{1}$$

$$\varepsilon = u' - \frac{w}{R}, \qquad \gamma = w' + \frac{u}{R} + \varphi, \qquad \chi = \varphi', \tag{2}$$

$$N = EA\varepsilon, \qquad T = GA_T\gamma, \qquad M = EI\chi. \tag{3}$$

Here, N, T and M denote the generalized stresses (axial and shear force and bending moment, see Figure 1 for the definition of positive quantities) and q_t, q_r and m the generalized external forces per unit length (tangent and radial forces and distributed couple moments). In the local reference system u and w are the displacements of the axis line and φ the section rotation while ε, γ and χ denote the generalized strains (axial, shear and curvature bending). Finally, symbols E, G, A, A_T and I indicate, respectively, the Young's modulus, the shear modulus, the cross-section area, the shear reduced cross-section and the area moment of inertia. The curved beam problem can be set in an equivalent variational formulation, such as the classical principle of total potential energy, which is certainly more suitable for a solution strategy based on finite elements:

$$\arg\min_{u,w,\varphi} \left\{ \frac{1}{2} \int_0^\ell (EA\varepsilon^2 + EI\chi^2 + GA_T\gamma^2) ds - \int_0^\ell (q_t u + q_r w + m\varphi) ds \right\}. \tag{4}$$

As a first step in order to discretize (4), we describe the geometry of a curved beam by means of NURBS interpolation (for a complete and more

Please cite this document as: A. Cazzani, M. Malagú, and E. Turco "Isogeometric analysis of plane–curved beams" *Mathematics and Mechanics of Solids*, 2016, 21(5): 562–577 DOI:10.1177/1081286514531265

accurate description of this kind of interpolation we refer to specialized books, [16]).

We say that $\mathbf{x}$ has a p-degree NURBS representation when there exist $n \in \mathbb{N}$, control points $\mathbf{P}_i \in \mathbb{R}^2$, weights $g_i \in \mathbb{R}$, $i = 1...n$, and a *knot vector*, i.e. a set $\boldsymbol{\Xi} = \{0 = \xi_1 \leq \xi_2 \leq ... \leq \xi_{n+p+1} = 1\}$ such that, for any $\xi \in [0; 1]$:

$$\mathbf{x}(\xi) = \sum_{i=1}^{n} R_{i,p}(\xi)\mathbf{P}_i, \tag{5}$$

where the NURBS basis $\{R_{i,p}(\xi)\}$ can be expressed as:

$$R_{i,p}(\xi) = \frac{B_{i,p}(\xi)g_i}{\sum_{i=1}^{n} B_{i,p}(\xi)g_i}, \tag{6}$$

in terms of B-splines bases $\{B_{i,p}(\xi)\}$ defined by the Cox-De Boor recursive formula:

$$B_{i,0}(\xi) = \begin{cases} 1 & \text{if} \quad \xi_i \leq \xi < \xi_{i+1} \\ 0 & \text{otherwise} \end{cases}, \tag{7}$$

$$B_{i,p}(\xi) = \frac{\xi - \xi_i}{\xi_{i+p} - \xi_i} B_{i,p-1}(\xi) + \frac{\xi_{i+p+1} - \xi}{\xi_{i+p+1} - \xi_{i+1}} B_{i+1,p-1}(\xi). \tag{8}$$

The so-called knot vector $\boldsymbol{\Xi}$ defines a partition of the parameter space $[0; 1]$ similar to the classic finite element subdivision. Non-uniform knot vectors and repeated knots are the key ingredients of NURBS flexibility and produce refined geometric descriptions. Weights g_i related to i-th control point enlarge the capabilities of the B-splines interpolation allowing also an exact representation of conic sections.

Among all the properties of NURBS interpolation the most interesting is the high-degree of continuity. More precisely, each p-th order function is of class C^{p-1}, i.e. it is continuous with its derivatives up to the $(p-1)$-th order, and in particular it is smooth across the boundaries. However, if necessary, continuity degree can also be lowered by using repeated knots.

The main idea of the isogeometric approach is to exactly describe the geometry of the problem by NURBS interpolation and to use the same interpolating basis to represent the generalized displacements:

$$u(\xi) \approx \sum_{i=1}^{n} R_{i,p}(\xi)u_i, \qquad w(\xi) \approx \sum_{i=1}^{n} R_{i,p}(\xi)w_i, \qquad \varphi(\xi) \approx \sum_{i=1}^{n} R_{i,p}(\xi)\varphi_i, \tag{9}$$

Please cite this document as: A. Cazzani, M. Malagú, and E. Turco "Isogeometric analysis of plane–curved beams" *Mathematics and Mechanics of Solids*, 2016, 21(5): 562–577 DOI:10.1177/1081286514531265

by means of control points u_i, w_i, and φ_i.

Using the dot to denote the derivatives with respect to ξ and denoting by J the Jacobian of the transformation, we have:

$$J = \dot{s} = \sqrt{\dot{x}_1^2 + \dot{x}_2^2}, \qquad R = \frac{J^3}{|\dot{x}_1\ddot{x}_2 - \ddot{x}_1\dot{x}_2|}, \tag{10}$$

thus, the generalized strains take the form:

$$\varepsilon = \frac{\dot{u}}{J} - \frac{w}{R}, \qquad \gamma = \frac{\dot{w}}{J} + \frac{u}{R}, \qquad \chi = \frac{\dot{\varphi}}{J}. \tag{11}$$

By using the position:

$$\begin{aligned} \pi_e &= \frac{1}{2}\int_{\xi_e}^{\xi_{e+1}} (EA\varepsilon^2 + EI\chi^2 + GA_T\gamma^2) J d\xi, \\ \lambda_e &= \int_{\xi_e}^{\xi_{e+1}} (q_t u + q_r w + m\varphi) J d\xi, \end{aligned} \tag{12}$$

problem (4) can now be discretized as:

$$\arg\min_{u,w,\varphi} \left\{ \sum_{e=1}^{n_e} \pi_e - \lambda_e \right\}. \tag{13}$$

where n_e is the number of subdivision of the parameter space. Imposing (13) produces a linear system of equations where the unknowns are the control points u_i, w_i e φ_i.

To set up the stiffness matrix and the load vector it is necessary to evaluate the integrals: this can be performed numerically by using the Gauss quadrature rule, even if the integrand functions are somewhat different from polynomials. By referring to [3] for some guidelines about the number of Gauss points to be used for an efficient quadrature, here we resort to a simple rule suggested by some numerical tests and validated by the numerical results presented in the next section. This is also useful to prevent locking problems such as described in [15].

3. Numerical results

In this section we present a series of numerical tests devoted to explore the performances of the proposed isogeometric finite element family. Their

Please cite this document as: A. Cazzani, M. Malagú, and E. Turco "Isogeometric analysis of plane–curved beams" *Mathematics and Mechanics of Solids*, 2016, 21(5): 562–577 DOI:10.1177/1081286514531265

results are compared with analytical solution, classical Lagrangian compatible elements, and some special (i.e. mixed or hybrid) finite elements reported in technical literature.

Comparison with reference solutions is particularly devoted to:

- asses the convergence rate of the proposed element also by comparison with classical elements such as those belonging to the Lagrangian family;
- test the influence of locking phenomena (if any);
- check these results against those produced by special elements particularly effective for curved beams;
- explore influence of the Gauss point number on the numerical results;
- make a critical analysis of the results produced by the NURBS element family devoted to select the most effective order.

All the numerical tests are built by using an *ad hoc* developed code which is essentially based on NURBS algorithms reported in [16] and coded in a NURBS library and on the GeoPDEs library of [17].

3.1. Tests devoted to calibrate the numerical model

Following the guidelines developed in [3] and bearing in mind the observation reported in [15], we consider the simple numerical tests reported in Figure 2. For both tests a reference solution is easy to evaluate. Furthermore, the first is a pure bending problem and the second a pure extensional problem. So they can use to highlight possible locking problems.

First, we consider the cantilever circular arch sketched in Figure 2(a). For this case, where the only generalized stress different from zero is the bending moment, the reference solution can be easily computed. In particular the free end vertical displacement is:

$$f = \frac{WR^2}{EI}, \tag{14}$$

where symbols which are not shown in Figure 2 are the Young's modulus, E, and the area moment of inertia of the cross-section, I.

Table 1 reports the free end vertical displacement by keeping fixed the number of elements, $n_e = 8$, and varying both the NURBS order p and the

Please cite this document as: A. Cazzani, M. Malagú, and E. Turco "Isogeometric analysis of plane–curved beams" *Mathematics and Mechanics of Solids*, 2016, 21(5): 562–577 DOI:10.1177/1081286514531265

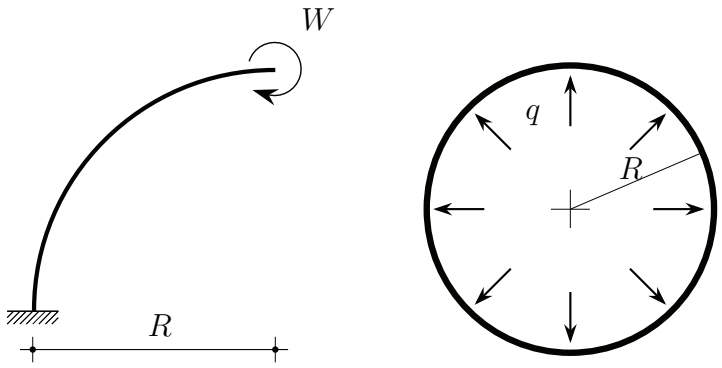

(a) Pure bending (b) Pure extension

Figure 2: Sketch of cantilever circular arch subjected to a couple at the free end and of ring under internal pressure.

Gauss points number n_g in the range $p, \ldots, 4p$. Reference value is obtained for a rectangular cross-section with thickness b=0.2 m, depth h=0.01 m, and unitary values for W, R, E, i.e.: W=1 Nm, R=1 m, E=1 GPa.

These results suggest that a number of Gauss points n_g equal to the NURBS order p is the best choice, since it furnishes accurate results with a low computational cost. Finally, we noticed that when $n_g < p$, i.e. the number of Gauss points is less than the NURBS order, some ill-conditioning of the stiffness matrix occurs, in particular for higher values of p. Therefore, for the sake of conciseness, only values of $n_g \geq p$ have been shown in Table 1. Moreover, unless otherwise noticed, the choice $n_g = p$ has been adopted for all tests, whose results are shown in the sequel.

Table 1: Cantilever circular arch subjected to a couple at the free end: vertical displacement of the free end by varying the NURBS order p and the number of Gauss points n_g ($n_e = 8$, reference value of the vertical displacement $f = 6$ cm).

	n_g			
p	p	$p+1$	$2p$	$4p$
2	5.9975	4.7793	4.7806	4.7806
3	5.9996	5.9994	5.9994	5.9994
4	5.9999	5.9999	5.9999	5.9999
5	5.9999	5.9999	5.9999	5.9999

Please cite this document as: A. Cazzani, M. Malagú, and E. Turco "Isogeometric analysis of plane–curved beams" *Mathematics and Mechanics of Solids*, 2016, 21(5): 562–577 DOI:10.1177/1081286514531265

Table 2 is again referred to the test reported in Figure 2(a) and reports the numerical solution for the vertical displacement f of the free end; this time it is either the number of elements, n_e, or the NURBS order, p, which is going to be increased. Besides the accuracy of the results, it is worth noticing that the computational cost is essentially linked to the number of degrees of freedom (dofs) of the problem. Since n_e elements of order p give $3(n_e + p)$ dofs, it is interesting to compare results having the same computational cost, i.e. by keeping fixed the value of $n_e + p$. We point out, to this end, that increasing the order p produces better results than increasing n_e.

Table 2: Cantilever circular arch subjected to a couple at the free end: vertical displacement f of the free end for different number of elements n_e and NURBS order p (reference value $f = 6$ cm). The adopted number of Gauss points is, in all shown cases, $n_g = p$.

	p			
n_e	2	3	4	5
4	5.9565	5.9852	5.9991	5.9999
8	5.9975	5.9996	5.9999	5.9999
16	5.9998	5.9999	5.9999	5.9999
32	5.9999	5.9999	5.9999	5.9999

Keeping in mind the observations reported in [15], we consider for the same test the vertical displacement f as a function of the R/h ratio and the NURBS order p, but keeping fixed the number of elements: in this case $n_e = 8$, see Table 3. We note that the results for low NURBS order p are poor when the R/h ratio increases and this is a symptom of the occurrence of locking. To better investigate this phenomenon, the behaviour of 2nd- and 3rd-order NURBS for the case $R/h = 10^4$ and $R/h = 10^5$ has been studied by increasing n_e. From Table 4 we deduce that also in this extreme cases, convergence is recovered by simply increasing n_e.

As a second test we choose the ring under internal pressure depicted in Figure 2(b). In this case, the only non-zero generalized stress component is the axial force N. Thanks to the polar symmetry it is straightforward to evaluate the reference solution. In particular, the axial force N_{ref} and the

Please cite this document as: A. Cazzani, M. Malagú, and E. Turco "Isogeometric analysis of plane–curved beams" *Mathematics and Mechanics of Solids*, 2016, 21(5): 562–577 DOI:10.1177/1081286514531265

Table 3: Cantilever circular arch subjected to a couple at the free end: vertical displacement f of the free end, scaled by the reference solution, varying R/h ratio and NURBS order p ($n_e = 8$).

	p			
R/h	2	3	4	5
10^2	0.99958	0.99993	0.99998	0.99998
10^3	0.98815	0.99660	0.99995	0.99998
10^4	0.49402	0.86520	0,99702	0.99997
10^5	0.00968	0.06190	0.98163	0.99912

Table 4: Cantilever circular arch subjected to a couple at the free end: vertical displacement f of the free, scaled by the reference solution, varying n_e for $R/h = 10^4$. and $R/h = 10^5$ ($p = 2$ and $p = 3$; $n_g = p$).

		p	
R/h	n_e	2	3
10^4	16	0.98163	0.99500
	32	0.99910	0.99985
	64	0.99997	0.99998
10^5	16	0.37252	0.79427
	32	0.97168	0.99198
	64	0.99902	0.99838

radial displacement w_{ref} are given by:

$$\begin{aligned} N_{\text{ref}} &= qR, \\ w_{\text{ref}} &= \frac{qR^2}{EA}. \end{aligned} \tag{15}$$

In Table 5 the radial displacement w and the axial force N are reported versus p and n_e (the number of elements being referred to a quarter of the whole ring). Both values of w and N are scaled by the reference solution. The results are relative to the following set of data: $q = 1$ kN/m, $R = 1$ m, $E = 1$ GPa and $A = 1$ cm^2.

First, also for this test the influence of the number of Gauss points has been investigated. The results confirm that $n_g = p$ is again the best choice,

Please cite this document as: A. Cazzani, M. Malagú, and E. Turco "Isogeometric analysis of plane–curved beams" *Mathematics and Mechanics of Solids*, 2016, 21(5): 562–577 DOI:10.1177/1081286514531265

even though they are not reported here for space-saving reasons. Successively, the accuracy of the results has been checked by computing N and w (properly scaled by the reference solutions) as a function of the number of elements, n_e, and of the NURBS order, p.

Again, as in the previous test, the conclusion is that the effect of the so-called p-refinement (i.e. increasing p) produces better results than the h-refinement (corresponding to increasing the number of elements, n_e). Indeed a relatively poor mesh can provide accurate results as long as p is suitably increased.

Table 5: Ring under internal pressure: radial displacement w and axial force N (both scaled for the reference solution) varying the number of element n_e and NURBS order p.

	p							
	2		3		4		5	
n_e	w/w_{ref}	N/N_{ref}	w/w_{ref}	N/N_{ref}	w/w_{ref}	N/N_{ref}	w/w_{ref}	N/N_{ref}
2	0.99816	1.0035	1.0000	1.0000	0.99824	1.0000	1.0000	1.0000
4	0.99464	1.0012	0.99981	1.0000	0.99999	1.0000	1.0000	1.0000
8	0.99601	1.0002	1.0000	1.0000	1.0000	1.0000	1.0000	1.0000
16	0.99971	1.0000	1.0000	1.0000	1.0000	1.0000	1.0000	1.0000
32	0.99998	1.0000	1.0000	1.0000	1.0000	1.0000	1.0000	1.0000

We point out that convergence is not uniform: this comes out by the k-refinement scheme implemented in our code for obtaining the numerical results. This kind of refinement, which is typical of isogeometric analysis, is different from the h- and p-refinement schemes of classical finite elements; see [1] and [18] for details.

Remembering the foregoing test and the loss of accuracy for small values of n_e and p, we also control the accuracy when the R/h ratio increases. Table 6 reports the radial displacement w and the axial force N, both scaled for the respective reference values, for the $2nd$-order NURBS and $n_e = 4$, when the R/h ratio varies in the range $10^2, \ldots, 10^5$. In this case there is no loss of accuracy, even for high values of R/h.

3.2. Cantilever circular arch under shear load at the free end

As a third test we consider the cantilever circular arch, see Figure 3, loaded with a vertical unit force P (in N) acting on the free end. We further

Please cite this document as: A. Cazzani, M. Malagú, and E. Turco "Isogeometric analysis of plane–curved beams" *Mathematics and Mechanics of Solids*, 2016, 21(5): 562–577 DOI:10.1177/1081286514531265

Table 6: Ring under internal pressure: radial displacement w and axial force N (both scaled for the reference solution) at varying R/h values for NURBS order $p = 2$ ($n_e = 4$).

	R/h			
	10^2	10^3	10^4	10^5
w/w_{ref}	0.99464	0.99429	0.99429	0.99426
N/N_{ref}	1.0012	1.0013	1.0013	1.0013

assume the values $R = 2$ m for the arc radius, $E = 80$ GPa for the Young's modulus, $\nu = 0.2$ for the Poisson's ratio. Finally, a rectangular cross-section with tickness $b = 0.2$ m and depth $h = 0.01$ m is considered.

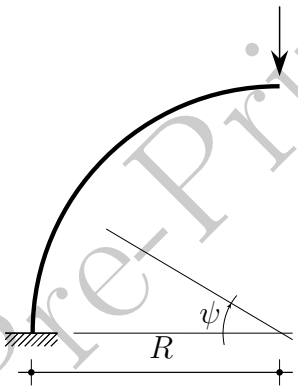

Figure 3: Sketch of the cantilever arch under shear load.

Also in this case, reference solution can easily be calculated and written as:

$$u = -P(c_1(\sin\psi + \psi\cos\psi) + c_2\sin\psi), \quad w = Pc_1\psi\sin\psi, \quad \varphi = -Pc_3\sin\psi, \tag{16}$$

where u, w, and φ are the tangential displacement, the radial displacement and the cross-section rotation, respectively, expressed in terms of the angle $\psi = s/R$ (see again Figure 3) and of the following compliance coefficients:

$$c_1 = \frac{1}{2}\left(\frac{R}{EA} + \frac{R}{GA_T} + \frac{R^3}{EI}\right), \qquad c_2 = \left(\frac{R}{GA_T} + \frac{R^3}{EI}\right), \qquad c_3 = \frac{R^2}{EI}. \tag{17}$$

Please cite this document as: A. Cazzani, M. Malagú, and E. Turco "Isogeometric analysis of plane–curved beams" *Mathematics and Mechanics of Solids*, 2016, 21(5): 562–577 DOI:10.1177/1081286514531265

Generalized stresses N, T and M and strain energy $\Phi = \frac{1}{2}Pw|_{\pi/2}$, assume the values:

$$N = -P\cos\psi, \qquad T = P\sin\psi, \qquad M = -PR\cos\psi, \qquad \Phi = \frac{1}{2}P^2 c_1 \frac{\pi}{2}. \tag{18}$$

In Table 7 the vertical displacement $f = w|_{\pi/2}$ of the free end as a function of the NURBS order p and the number of elements n_e is reported. Even in this case, if we compare analyses performed with the same computational cost, i.e. with the same value of $n_e + p$, it comes out that the higher the degree p, the better the result is.

Table 7: Cantilever arch under shear load: vertical displacement f of the free end as a function of the element number n_e and NURBS order p (reference value=4.7124 mm).

	p			
n_e	2	3	4	5
1	4.4665	4.7059	4.7120	4.7124
2	3.8229	3,4257	4.6090	4.7080
4	3.8794	4.5343	4.7059	4.7122
8	4.6329	4.7076	4.7124	4.7124
16	4.7108	4.7124	4.7124	4.7124
32	4.7124	4.7124	4.7124	4.7124

Table 8 reports the only non-zero reactions at the clamped end: the vertical force V_A and bending moment M_A for various NURBS order p and element number n_e. Naturally, since our NURBS elements are based on a displacement-type compatible formulation, it is expected that stress quantities exhibit relatively poor performances; nonetheless good results can be obtained even with few elements by suitably increasing the NURBS order p.

In order to compare the performances of NURBS to those of classical Lagrangian interpolation, we report in Table 9 the vertical displacement of the free end f and the reactions at the clamped end V_A and M_A for different order p and number of element n_e. We notice the superior computational performances of NURBS interpolation with reference to the Lagrangian one.

Please cite this document as: A. Cazzani, M. Malagú, and E. Turco "Isogeometric analysis of plane–curved beams" *Mathematics and Mechanics of Solids*, 2016, 21(5): 562–577 DOI:10.1177/1081286514531265

Table 8: Cantilever arch under shear load: reactions at the clamped end vs. the element number n_e and NURBS order p.

p	n_e	V_A [N]	M_A [Nm]
2	16	4.1624	2.0008
	32	1.7861	2.0001
	64	1.1960	2.0000
3	8	0.78097	1.9992
	16	0.97405	1.9999
	32	0.99680	2.0000
	64	0.99960	2.0000
4	4	1.1809	1.9945
	8	1.0044	2.0000
	16	1.0001	2.0000
	32	1.0000	2.0000
	64	1.0000	2.0000
5	2	1.5499	1.9861
	4	1.0041	2.0015
	8	0.99903	2.0000
	16	0.99997	2.0000
	32	1.0000	2.0000
	64	1.0000	2.0000
analytical		1	2

3.3. Incomplete ring under vertical load

This numerical test was chosen since it allows a comparison with a large number of finite elements reported in technical literature. According to [19] and later [20], the problem sketched in Figure 4 was analyzed using these data: load $P = 1$ lb; radius $R = 2.935$ in; Young's modulus $E = 1.05 \times 10^7$ psi; Poisson's ratio $\nu = 0.3$; rectangular cross-section with thickness $b = 1.2$ in and depth $h = 0.125$ in.

For this test we have also computed the analytical solution by integrating the system of six linear first-order ODEs resulting from (1)–(3) and properly enforcing the boundary conditions (BCs), account taken of symmetry with reference to the vertical axis. The generalized stresses N, T, M are given by

Please cite this document as: A. Cazzani, M. Malagú, and E. Turco "Isogeometric analysis of plane–curved beams" *Mathematics and Mechanics of Solids*, 2016, 21(5): 562–577 DOI:10.1177/1081286514531265

Table 9: Cantilever arch under shear load: vertical displacement f of the free end and reaction components V_A and M_A at the clamped end as a function of the element number n_e and of the order of Lagrangian interpolation p_L.

p_L	n_e	f [mm]	V_A [N]	M_A [Nm]
2	16	4.1337	320.22	1.6637
	32	4.6685	96.007	1.9737
	64	4.7098	25.068	1.9984
3	8	4.7087	0.83102	2.0124
	16	4.7116	0.97569	2.0026
	32	4.7122	0.99862	2.0005
	64	4.7124	0.99994	2.0001
4	4	4.7124	8.5569	2.0116
	8	4.7124	0.18327	2.0003
	16	4.7124	0.94724	2.0000
	32	4.7124	0.99669	2.0000
	64	4.7124	0.99979	2.0000
5	2	4.7126	0.29883	1.9959
	4	4.7124	1.0093	1.9999
	8	4.7124	1.0003	2.0000
	16	4.7124	1.0000	2.0000
	32	4,7124	1.0000	2.0000
	64	4.7124	1.0000	2.0000
analytical		4.7124	1	2

(see again Figure 4 for the definition of the angle ψ):

$$\begin{aligned} N =& A_1 \cos\psi + A_2 \sin\psi, \\ T =& A_2 \cos\psi - A_1 \sin\psi, \\ M =& A_2 R \sin\psi - A_1 R(1-\cos\psi) + A_3, \end{aligned} \tag{19}$$

while the tangential and radial displacement and the cross-section rotation

Please cite this document as: A. Cazzani, M. Malagú, and E. Turco "Isogeometric analysis of plane–curved beams" *Mathematics and Mechanics of Solids*, 2016, 21(5): 562–577 DOI:10.1177/1081286514531265

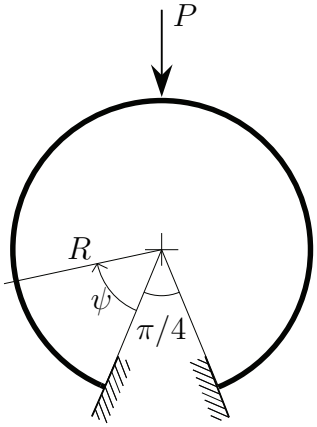

Figure 4: Sketch of incomplete ring under vertical load.

are:

$$\begin{aligned} u =& A_1[c_1(\psi\cos\psi+\sin\psi)-c_2\sin\psi-c_3R(\sin\psi-\psi)]+\\ & A_2[c_1\psi\sin\psi-c_3R(1-\cos\psi)]+A_3c_3(\sin\psi-\psi),\\ w =& A_2[c_1(\psi\cos\psi-\sin\psi)+c_2\sin\psi-c_3R\sin\psi]-\\ & A_1[c_1\psi\sin\psi-c_3R(1-\cos\psi)]-A_3c_3(1-\cos\psi),\\ \varphi =& A_1c_3(\sin\psi-\psi)+A_2c_3(1-\cos\psi)+A_3c_3\psi/R. \end{aligned} \tag{20}$$

In (20) the same compliance coefficients c_1, c_2, c_3 defined in (17) are used as a short-hand notation, while constants A_1, A_2 and A_3 appearing in (19)–(20) assume these values:

$$\begin{aligned} A_1 =& -\frac{2P[c_1(\alpha^2/R)-c_3(1-\cos\alpha)]\sin\alpha}{4c_1(\alpha^2/R)-2c_3(1-\cos2\alpha)+2\alpha\sin2\alpha(c_1/R-c_2/R+c_3)},\\ A_2 =& \frac{2P[c_1(\alpha/R)(\alpha\cos\alpha+\sin\alpha)-c_2(\alpha/R)\sin\alpha-c_3\sin\alpha(\sin\alpha-\alpha)]}{4c_1(\alpha^2/R)-2c_3(1-\cos2\alpha)+2\alpha\sin2\alpha(c_1/R-c_2/R+c_3)},\\ A_3 =& \frac{2P[c_1\alpha(1-\cos\alpha-\alpha\sin\alpha)+(c_1-c_2)\sin\alpha(\cos\alpha-1)]}{4c_1(\alpha^2/R)-2c_3(1-\cos2\alpha)+2\alpha\sin2\alpha(c_1/R-c_2/R+c_3)}. \end{aligned} \tag{21}$$

Setting $\alpha = 7\pi/8$, for the given data the vertical displacement f of the incomplete ring middle point results in $f = 1.063161841\times10^3$ when all strain contributions are taken into account; on the other hand, if shear deformation is discarded $f|_{\gamma=0} = 1.059622233\times10^3$, while if both extensional and

Please cite this document as: A. Cazzani, M. Malagú, and E. Turco "Isogeometric analysis of plane–curved beams" *Mathematics and Mechanics of Solids*, 2016, 21(5): 562–577 DOI:10.1177/1081286514531265

shear deformation are disregarded it results $f|_{\gamma=0;\epsilon=0} = 1.058121422 \times 10^3$. The analytic solution provided by [19], $f = 1.06364 \times 10^3$, does not seem compatible with the assumed geometric and mechanical data.

Table 10 reports the vertical displacement f under the unitary load varying the NURBS order p and the numbers of element n_e on one-half of the structure. In the same Table are reported both the analytical solution and the results obtained in [19] and [20] with several type of finite elements. In order to simplify the comparison, a column with the number of nodes n_n is also reported. The Table shows the good performances of the NURBS element family.

Table 10: Incomplete ring under vertical load: middle point vertical displacement f.

p	n_e	n_n	$f \times 10^{-3}$	Formulation	Geometry
	8	10	0.99727	compatibility	exact
2	16	18	1.06201	”	”
	32	34	1.06314	”	”
	8	11	1.05863	”	”
3	16	19	1.06311	”	”
	32	35	1.06316	”	”
	8	12	1.06301	”	”
4	16	20	1.06316	”	”
	32	36	1.06316	”	”
	8	13	1.06315	”	”
5	16	21	1.06316	”	”
	32	37	1.06316	”	”
analytical	—	—	1.06316	—	—
[19]	8	16	1.05641	compatibility	exact
[19]	8	16	1.05641	hybrid	exact
[19]	8	16	1.05619	mixed	exact
[20]	1	3	1.07069	equilibrium	cubic parametric
[20]	2	6	1.06384	equilibrium	cubic parametric

3.4. Clamped-clamped semi-circular arch under distributed load

Now, we consider the clamped-clamped semi-circular arch depicted in Figure 5. This time, we assume $R = 1$ m, a square cross-section with side

Please cite this document as: A. Cazzani, M. Malagú, and E. Turco “Isogeometric analysis of plane–curved beams” *Mathematics and Mechanics of Solids*, 2016, 21(5): 562–577 DOI:10.1177/1081286514531265

$b = 0.1$ m, Young's modulus $E = 1$ GPa, Poisson's ratio $\nu = 0$ and, finally, a load $q = 1$ N/m. The analytical solution is provided again by integrating the system (1)–(3), properly enforcing BCs and symmetry with reference to the vertical axis. In this case, by taking into account that the load is uniformly distributed per unit of projection, it results: $q_t = -q \sin\psi \cos\psi$ and $q_r = q \sin^2\psi$. The generalized stresses N, T, M and displacements u, w and φ are, respectively, given by:

$$\begin{aligned} N =& A_2 \sin\psi - qR\cos^2\psi, \\ T =& A_2 \cos\psi + qR\cos\psi\sin\psi, \\ M =& A_2 R\sin\psi + A_3 - qR^2/2(1 + 1/2\cos 2\psi), \end{aligned} \tag{22}$$

and

$$\begin{aligned} u =& A_2[c_1\psi\sin\psi - c_3R(1-\cos\psi)] - A_3c_3(\psi - \sin\psi) + \\ & A_5\sin\psi - qR[\sin 2\psi(2/3c_1 - 1/6c_2 - 1/8c_3R) - \psi c_3R/2], \\ w =& A_2[c_1(\psi\cos\psi - \sin\psi) + c_2\sin\psi - c_3R\sin\psi] - A_3c_3(1-\cos\psi) + \\ & A_5\cos\psi + qR[c_1 - 1/2c_2 + 1/2c_3R - \cos 2\psi(1/3c_1 + 1/6c_2 - 1/4c_3R)], \\ \varphi =& A_3\psi/Rc_3 - A_2c_3(\cos\psi - 1) - qRc_3(\psi/2 + 1/8\sin 2\psi). \end{aligned} \tag{23}$$

As before, in (23) the compliance coefficients c_1, c_2, c_3 defined in (17) have been used for brevity, while constants A_2, A_3 and A_5 appearing in (22)–(23) assume the values:

$$\begin{aligned} A_2 =& \frac{8\pi q(c_1 - c_2) + 3\pi qRc_3}{6\pi^2(c_1/R) - 24c_3}, \\ A_3 =& \frac{qR^2}{2} - \frac{16\pi qR(c_1 - c_2) + 6\pi qR^2c_3}{6\pi^3(c_1/R) - 24\pi c_3}, \\ A_5 =& -\frac{2qR(c_1 - c_2)}{3} - \frac{3qR^2c_3}{4}. \end{aligned} \tag{24}$$

For the given data, the vertical displacement of the arch middle point, evaluated in exact form with a Computer Algebra System is $v_C = 1.018188371$ mm when all strain contribution are taken into account; if shear deformation is discarded $v_C|_{\gamma=0} = 0.982381687$ mm, while if both extensional and shear deformation are disregarded it results $v_C|_{\gamma=0;\epsilon=0} = 0.817230149$ mm. The reactions at point A are instead: $H_A = 0.554438$ N, $V_A = 1.000000$ N and $M_A = 0.102966$ Nm.

Please cite this document as: A. Cazzani, M. Malagú, and E. Turco "Isogeometric analysis of plane–curved beams" *Mathematics and Mechanics of Solids*, 2016, 21(5): 562–577 DOI:10.1177/1081286514531265

We point out that some results of the analytical solution provided by [20], i.e. $v_C = 1.02086$ mm, $H_A = 0.554915$ N, $M_A = 0.103980$ Nm differ from the analytical solution presented above.

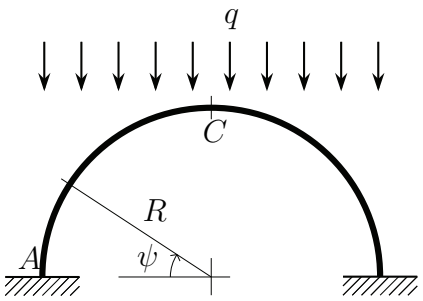

Figure 5: Sketch of the clamped-clamped semi-circular arch under distributed load.

Table 11 reports the values of the vertical displacement v_C of the point C and the reactions at the clamped end A: the horizontal, H_A, and vertical, V_A, force components and bending moment, M_A, for different NURBS order p and number of elements n_e (referred to one half of the arch), along with our analytical values. In the same table, the results obtained by [20] neglecting transverse shear deformation are reported.

We remark the high accuracy of our results, for both displacements and generalized stresses even if convergence rate for stresses is slower and a large number of elements or a higher NURBS degree is required to achieve a good quality approximation.

3.5. Three-hinged lancet arch under self weight

The three-hinged pointed arch reported in Figure 6 is taken into consideration with the following set of data: $E = 1$ GPa, $\nu = 0.2$, $R = 1$ m, $b = 0.2$ m, $h = 0.01$ m and $q_0 = 1$ kN/m.

As before, the analytical solution has been computed by integrating (1)–(3) and imposing the relative boundary and symmetry conditions. In particular at the arch tip, i.e. for $\alpha = \pi/4$, the following BCs, which involve the bending moment M, the horizontal displacement h, and the vertical component of the internal force V, must be met:

$$M|_\alpha = 0; \quad h|_\alpha = u|_\alpha \sin\alpha + w|_\alpha \cos\alpha = 0; \quad V|_\alpha = N|_\alpha \cos\alpha - T|_\alpha \sin\alpha = 0.$$

Since the load is uniformly distributed per unit of arc-length (and not per unit of projection), it results $q_t = -q_0 \cos\psi$ and $q_r = q_0 \sin\psi$. Then, the

Please cite this document as: A. Cazzani, M. Malagú, and E. Turco "Isogeometric analysis of plane–curved beams" *Mathematics and Mechanics of Solids*, 2016, 21(5): 562–577 DOI:10.1177/1081286514531265

Table 11: Clamped-clamped semi-circular arch under distributed load: middle vertical displacement and clamp reactions.

p	n_e	v_C [mm]	H_A [N]	V_A [N]	M_A [Nm]
2	16	1.01812	0.728620	0.932677	0.102130
	32	1.01819	0.598888	0.981880	0.102778
3	8	1.01811	0.571273	0.968679	0.103210
	16	1.01819	0.556235	0.996308	0.102981
	32	1.01819	0.554667	0.995452	0.102968
4	8	1.01819	0.553398	1.00105	0.102945
	16	1.01819	0.554405	1.00003	0.102966
	32	1.01819	0.554437	1.00000	0.102966
5	8	1.01819	0.554595	0.999814	0.102966
	16	1.01819	0.554440	0.999995	0.102966
	32	1.01819	0.554438	1.000000	0.102966
analytical	—	1.01819	0.554438	1	0.102966
[20]	1	1.02135	0.555009	1.0	0.104159
[20]	2	9.9091	0.500476	1.0	0.092636
[20]	4	1.00177	0.540775	1.0	0.101238

generalized stresses N, T, M are given by:

$$\begin{aligned} N &= A_1 \cos\psi + A_2 \sin\psi + q_0 R\psi \cos\psi, \\ T &= A_2 \cos\psi - A_1 \sin\psi - q_0 R\psi \sin\psi, \\ M &= A_1 R(\cos\psi - 1) + A_2 R \sin\psi + q_0 R^2(\psi \cos\psi - \sin\psi), \end{aligned} \tag{25}$$

Please cite this document as: A. Cazzani, M. Malagú, and E. Turco "Isogeometric analysis of plane–curved beams" *Mathematics and Mechanics of Solids*, 2016, 21(5): 562–577 DOI:10.1177/1081286514531265

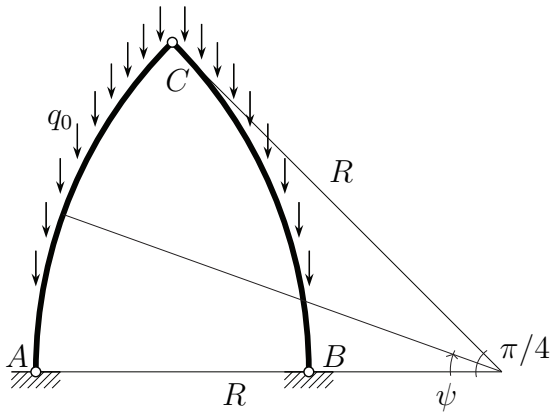

Figure 6: Sketch of the three-hinged lancet arch under self weight.

while displacements and cross-section rotation are:

$$\begin{aligned}
u =& A_1[c_1\psi\cos\psi + (c_1 - c_2 - c_3R)\sin\psi + c_3R\psi] + A_4\cos\psi + \\
& A_2[c_1\psi\sin\psi + c_3R(\cos\psi - 1)] + A_6R(\cos\psi - 1) + \\
& q_0[c_1R(\psi^2/2)\cos\psi + (c_1 - c_2)R(\cos\psi + 2\psi\sin\psi)/4 - \\
& \quad c_3R^2(2\cos\psi + \psi\sin\psi)], \\
w =& A_1[-c_1\psi\sin\psi + c_3R(1 - \cos\psi)] - A_4\sin\psi + \\
& A_2[c_1(\psi\cos\psi - \sin\psi) + c_2\sin\psi - c_3R\sin\psi] - A_6R\sin\psi + \\
& q_0[(c_2 - c_1)R(2\psi\cos\psi - \sin\psi)/4 - c_1R(\psi^2/2)\sin\psi + \\
& \quad c_3R^2(\sin\psi - \psi\cos\psi)], \\
\varphi =& A_1c_3(\sin\psi - \psi) + A_2c_3(1 - \cos\psi) + A_6 + q_0c_3R(2\cos\psi + \psi\sin\psi).
\end{aligned} \tag{26}$$

In (26) the compliance coefficients c_1, c_2, c_3 defined in (17) have been used to simplify notation, while constants A_1, A_2, A_4 and A_6 appearing in (25)–(26) assume these values:

$$\begin{aligned}
A_1 =& -q_0R\alpha, \\
A_2 =& q_0R(1 - \alpha/\sin\alpha), \\
A_4 =& q_0R[2c_3R + (c_2 - c_1)/4], \\
A_6 =& -q_0[c_1\alpha^2/\sin^2\alpha + (c_1 - c_2)(1/2\cos\alpha - \alpha/\tan\alpha) - \\
& \quad (c_1 + c_2)\alpha/(2\sin\alpha) + c_3R(1 + \alpha^2 + \alpha/\tan\alpha - \alpha/\sin\alpha + \cos\alpha)].
\end{aligned} \tag{27}$$

Please cite this document as: A. Cazzani, M. Malagú, and E. Turco "Isogeometric analysis of plane–curved beams" *Mathematics and Mechanics of Solids*, 2016, 21(5): 562–577 DOI:10.1177/1081286514531265

For the given data, the vertical displacement of the arch middle point, evaluated in exact form with a Computer Algebra System is $v_C = 5.47802398$ mm when all strain contribution are taken into account. The reactions at point A are instead: $H_A = 110.72073454$ N, $V_A = 785.39816340$ N.

Table 12 reports the values of the vertical displacement v_C and the reactions at support A, the horizontal, H_A, and the vertical, V_A, force components for different NURBS order p and number of element n_e (only one half of the arch was considered due to the symmetry).

Table 12: Three-hinged lancet arch under self weight: tip displacement and reaction forces at the support A.

p	n_e	v_C [mm]	H_A [kN]	V_A [kN]
2	32	5.47801	0.314991	0.790041
3	16	5.47800	0.146215	0.771868
	32	5.47802	0.114962	0.783706
	8	5.47802	0.115145	0.782591
4	16	5.47802	0.110882	0.785265
	32	5.47802	0.110727	0.785391
	8	5.47802	0.110620	0.785651
5	16	5.47802	0.110723	0.785402
	32	5.47802	0.110721	0.785398
analytical	—	5.47802	0.110721	0.785398

4. Concluding remarks

In this paper, NURBS finite elements for the analysis of plane curved beams have been investigated. Numerical results show, for this family of finite elements, good performances. In particular, accuracy and convergence ratio by varying both the number of elements and the NURBS order have been thoroughly studied. The influence of the number of Gauss points on the results was considered too, and a simple rule was proposed, which consists of using p Gauss points to integrate the stiffness matrix corresponding to a p-th order NURBS finite element. Besides numerical results, some new analytical solutions have been provided in order to expand those available in the technical literature. This paper has surely given some useful guidelines

Please cite this document as: A. Cazzani, M. Malagú, and E. Turco "Isogeometric analysis of plane–curved beams" *Mathematics and Mechanics of Solids*, 2016, 21(5): 562–577 DOI:10.1177/1081286514531265

about the isogeometric approach for plane curved beams but there are a few aspects which, in our opinion, deserve further extensions. What we consider the most interesting ones are listed below:

1. The first extension descends from observing the generalized stress results produced by the numerical model. Since they are clearly less accurate than the corresponding displacements, a possible improvement could be found in the framework of mixed formulations, like those proposed in [21], or in special stress recovery techniques (see [22]).
2. NURBS interpolation is somewhat different from polynomial interpolation, so that using the same integration rules, (i.e. standard Gauss formulae which rigorously apply only to polynomials) might not be the best way to obtain accurate results or the most suitable from the point of view of computational cost. Different solutions have been proposed, for example, in [23]. For these reasons, we think that this issue would require additional investigations.
3. Some possible applications of the Timoshenko beam model and non-classical applications of 1D beam-like model are worth mentioning. Among them there is the analysis of beams made of composite and functionally graded materials where proper relations for 1D elastic properties are established ([24]); the extension of the Timoshenko beam model to the thermal problems for beams within the framework of two temperature model ([25]); the description of particular phenomena like a line tension of phase interfaces in 2D structures such as a martensitic film ([26]).
4. The promising results obtained for plane curved beams suggest an extension to space-curved beams and also to more complicated two-dimensional structures such as shells. Moreover, extensions to investigate problems where both geometric and material nonlinearities can occur ([27]), or to linear and non-linear structural dynamics ([28], [29]) and buckling ([30], [31]) could be achieved, as well as the search for fundamental solutions through Green's operator ([32]).
5. Some applications require considering continuum models which are richer than the standard Cauchy one: it would be possible then trying to extend the proposed isogeometric approach to second and higher-order continua (see [33], [34], [35], [36]).
6. A foreseable application is the study of larger systems made of many NURBS special elements, for example for the analysis of damage me-

Please cite this document as: A. Cazzani, M. Malagú, and E. Turco "Isogeometric analysis of plane–curved beams" *Mathematics and Mechanics of Solids*, 2016, 21(5): 562–577 DOI:10.1177/1081286514531265

chanics in the framework of structural health monitoring (see [37], [38], [39], [40]) or along the statistical approach developed for Hookean spring networks (see [41], [42], [43]).

7. Finally, an interesting application would involve tackling composite or porous ([44]) or fibrous materials ([45]), even in cases when complex physical problems like bio-medical ones whose evolution is governed by integro-differential operators and material properties are subject to sudden changes ([46], [47], [48]). In all these cases it is believed that the ability of properly modulating the regularity of the basis function through the use of NURBS could make more tractable such problems.

Acknowledgements

The financial support of RAS, the Autonomous Region of Sardinia, under grant number F71J09999350002-CRP1_475 (Legge Regionale 7/2007, bando 2008, Progetto *MISC: Metodi Isogeometrici per Strutture Curve*) is gratefully acknowledged.

References

[1] T. J. R. Hughes, J. A. Cottrell, Y. Bazilevs, Isogeometric analysis: CAD, finite elements, NURBS, exact geometry and mesh refinement, Computer Methods in Applied Mechanics and Engineering 194 (2005) 4135–4195.

[2] J. A. Cottrell, T. J. R. Hughes, Y. Bazilevs, Isogeometric Analysis: Toward Integration of CAD and FEA, Wiley, 2009.

[3] T. J. R. Hughes, A. Reali, G. Sangalli, Efficient quadrature for NURBS-based isogeometric analysis, Computer Methods in Applied Mechanics and Engineering 199 (2010) 301–313.

[4] D. J. Benson, Y. Bazilevs, M. C. Hsu, T. J. R. Hughes, Isogeometric shell analysis: the Reissner-Mindlin shell, Computer Methods in Applied Mechanics and Engineering 199 (2010) 276–289.

[5] A. Benedetti, A. M. Tralli, A new hybrid F.E. model for arbitrarily curved beam–I. linear analysis, Computer and Structures 33 (1989) 1437–1449.

Please cite this document as: A. Cazzani, M. Malagú, and E. Turco "Isogeometric analysis of plane–curved beams" *Mathematics and Mechanics of Solids*, 2016, 21(5): 562–577 DOI:10.1177/1081286514531265

[6] C. Gontier, C. Vollmer, A large displacement analysis of a beam using a CAD geometric definition, Computer and Structures 57 (1995) 981–989.

[7] R. Echter, M. Bischoff, Numerical efficiency, locking and unlocking of NURBS finite elements, Computer Methods in Applied Mechanics and Engineering 199 (2010) 374–382.

[8] L. Beirão da Veiga, C. Lovadina, A. Reali, Avoiding shear locking for the Timoshenko beam problem via isogeometric collocation methods, Computer Methods in Applied Mechanics and Engineering 241–244 (2012) 38–51.

[9] F. Auricchio, L. Beirão da Veiga, J. Kiendl, C. Lovadina, A. Reali, Locking-free isogeometric collocation methods for spatial Timoshenko rods, Computer Methods in Applied Mechanics and Engineering 263 (2013) 113–126.

[10] M. Cuomo, L. Greco, Isogeometric analysis of space rods: considerations on stress locking, in: ECCOMAS 2012, 2012, pp. 1–19.

[11] L. Greco, M. Cuomo, B-Spline interpolation of Kirchhoff-Love space rods, Computer Methods in Applied Mechanics and Engineering 256 (2013) 251–269.

[12] L. Greco, M. Cuomo, A locking-free multipatch B-spline element for the analysis of curved 3D rod elements, in: Aimeta 2013, 2013, pp. 1–10.

[13] M. Cuomo, L. Contrafatto, L. Greco, A variational model based on isogeometric interpolation for the analysis of cracked bodies, International Journal of Engineering Sciences (2013) (in press).

[14] L. Greco, M. Cuomo, An implicit G^1 multi patch B-spline interpolation for Kirchhoff-Love space rods , Computer Methods in Applied Mechanics and Engineering 269 (2014) 173–197.

[15] R. Bouclier, T. Elguedj, A. Combescure, Locking free isogeometric formulations of curved thick beams, Computer Methods in Applied Mechanics and Engineering 245–246 (2012) 144–162.

[16] L. Piegl, W. Tiller, The NURBS Book, 2nd ed., Springer, 1996.

Please cite this document as: A. Cazzani, M. Malagú, and E. Turco "Isogeometric analysis of plane–curved beams" *Mathematics and Mechanics of Solids*, 2016, 21(5): 562–577 DOI:10.1177/1081286514531265

[17] C. de Falco, A. Reali, R. Vazquez, GeoPDEs: a research tool for isogeometric analysis of PDEs, Advances in Engineering Software 42 (2011) 1020–1034.

[18] J. A. Cottrell, T. J. R. Hughes, A. Reali, Studied of refinement and continuity in isogeometric structural analysis, Computer Methods in Applied Mechanics and Engineering 196 (2007) 4160–4183.

[19] H. Stolarski, T. Belytschko, Shear and membrane locking in curved C^0 elements, Computer Methods in Applied Mechanics and Engineering 41 (1983) 279–296.

[20] L. Molari, F. Ubertini, A flexibility-based element for linear analysis of arbitrarily curved arches, International Journal for Numerical Methods in Engineering 65 (2006) 1333–1353.

[21] M. Cuomo, G. Ventura, Complementary energy approach to contact problems based on consistent augmented Lagrangian formulation, Mathematical and Computer Modelling 28 (1998) 185–204.

[22] D. Ciancio, I. Carol, M. Cuomo, On inter-element forces in the FEM-displacement formulation, and implications for stress recovery, International Journal for Numerical Methods in Engineering 66 (2006) 502–528.

[23] M. J. Borden, M. A. Scott, J. A. Evans, T. J. R. Hughes, Isogeometric finite element data structures based on Bézier extraction of NURBS, International Journal for Numerical Methods in Engineering 87 (2011) 15–47.

[24] M. Bîrsan, H. Altenbach, T. Sadowski, V. Eremeyev, D. Pietras, Deformation analysis of functionally graded beams by the direct approach, Composites Part B: Engineering 43 (2012) 1315–1328.

[25] H. Altenbach, M. Bîrsan, V. A. Eremeyev, On a thermodynamic theory of rods with two temperature fields, Acta Mechanica 223 (2012) 1583–1596.

[26] W. Pietraszkiewicz, V. Eremeyev, V. Konopińska, Extended non-linear relations of elastic shells undergoing phase transitions, ZAMM—Zeitschrift für Angewandte Mathematik und Mechanik 87 (2007) 150–159.

Please cite this document as: A. Cazzani, M. Malagú, and E. Turco "Isogeometric analysis of plane–curved beams" *Mathematics and Mechanics of Solids*, 2016, 21(5): 562–577 DOI:10.1177/1081286514531265

[27] G. Oliveto, M. Cuomo, Incremental analysis of plane frames with geometric and material nonlinearities, Engineering Structures 10 (1988) 2–12.

[28] A. Luongo, G. Rega, F. Vestroni, On nonlinear dynamics of planar shear indeformable beams, Journal of Applied Mechanics, Transactions ASME 53 (1986) 619–624.

[29] A. D. Egidio, A. Luongo, A. Paolone, Linear and non-linear interactions between static and dynamic bifurcations of damped planar beams, International Journal of Non-Linear Mechanics 42 (2007) 88–98.

[30] A. Luongo, On the amplitude modulation and localization phenomena in interactive buckling problems, International Journal of Solids and Structures 27 (1991) 1943–1954.

[31] A. Luongo, Mode localization in dynamics and buckling of linear imperfect continuous structures, Nonlinear Dynamics 25 (2001) 133–156.

[32] M. Cuomo, G. Ventura, An explicit formulation of the Green's operator for general one-dimensional structures, European Journal of Mechanics, A/Solids 21 (2002) 493–512.

[33] F. dell'Isola, G. Ruta, R. Batra, Second-order solution of Saint-Venant's problem for an elastic pretwisted bar using Signorini's perturbation method, Journal of Elasticity 49 (1997) 113–127.

[34] R. Batra, F. dell'Isola, S. Vidoli, A second-order solution of Saint-Venant's problem for a piezoelectric circular bar using Signorini's perturbation method, Journal of Elasticity 52 (1998) 75–90.

[35] J.-J. Alibert, P. Seppecher, F. dell'Isola, Truss modular beams with deformation energy depending on higher displacement gradients, Mathematics and Mechanics of Solids 8 (2003) 51–73.

[36] F. dell'Isola, P. Seppecher, A. Madeo, How contact interactions may depend on the shape of Cauchy cuts in N-th gradient continua: Approach *à la D'Alembert*, ZAMP—Zeitschrift für Angewandte Mathematik und Physik 63 (2012) 1119–1141.

Please cite this document as: A. Cazzani, M. Malagú, and E. Turco "Isogeometric analysis of plane–curved beams" *Mathematics and Mechanics of Solids*, 2016, 21(5): 562–577 DOI:10.1177/1081286514531265

[37] N. Roveri, A. Carcaterra, Damage detection in structures under traveling loads by Hilbert-Huang transform, Mechanical Systems and Signal Processing 28 (2012) 128–144.

[38] N. Roveri, A. Carcaterra, Structural health monitoring of time-varying systems by output-only identification, in: Proceedings of ISMA 2012, International Conference on Noise and Vibration Engineering, KU Leuven, Leuven, 2012. ISBN: 9789073802896.

[39] N. Roveri, A. Carcaterra, A. Sestieri, Integrated system for shm and wear estimation of railway infrastructures, in: Surveillance 7 — 7th International Conference on Acoustical and Vibratory Surveillance Methods and Diagnostic Techniques, Chartres, 2013, pp. P39/1–19.

[40] A. Sestieri, A. Carcaterra, N. Roveri, New monitoring technologies in mechanical systems, in: Surveillance 7 — 7th International Conference on Acoustical and Vibratory Surveillance Methods and Diagnostic Techniques, Chartres, 2013, pp. P4/1–21.

[41] A. Rinaldi, Y.-C. Lai, Statistical damage theory of 2D lattices: Energetics and physical foundations of damage parameter, International Journal of Plasticity 23 (2007) 1796–1825.

[42] A. Rinaldi, Rational damage model of 2D disordered brittle lattices under uniaxial loadings, International Journal of Damage Mechanics 18 (2009) 233–257.

[43] A. Rinaldi, L. Placidi, A microscale second gradient approximation of the damage parameter of quasi-brittle heterogeneous lattices, ZAMM—Zeitschrift für Angewandte Mathematik und Mechanik (2013) 1–16. DOI:10.1002/zamm.201300028.

[44] A. Madeo, F. dell'Isola, F. Darve, A continuum model for deformable, second gradient porous media partially saturated with compressible fluids, Journal of the Mechanics and Physics of Solids 61 (2013) 2196–2211.

[45] M. Ferretti, A. Madeo, F. dell'Isola, P. Boisse, Modeling the onset of shear boundary layers in fibrous composite reinforcements by second-gradient theory, ZAMP—Zeitschrift für Angewandte Mathematik und Physik (2013) 1–26. DOI:10.1007/s00033-013-0347-8.

Please cite this document as: A. Cazzani, M. Malagú, and E. Turco "Isogeometric analysis of plane–curved beams" *Mathematics and Mechanics of Solids*, 2016, 21(5): 562–577 DOI:10.1177/1081286514531265

[46] A. Madeo, T. Lekszycki, F. dell'Isola, A continuum model for the biomechanical interactions between living tissue and bio-resorbable graft after bone reconstructive surgery, Comptes Rendus Mécanique 339 (2011) 625–640.

[47] T. Lekszycki, F. dell'Isola, A mixture model with evolving mass densities for describing synthesis and resorption phenomena in bones reconstructed with bio-resorbable materials, ZAMM—Zeitschrift für Angewandte Mathematik und Mechanik 92 (2012) 426–444.

[48] A. Madeo, D. George, T. Lekszycki, M. Nierenberger, Y. Rémond, A second gradient continuum model accounting for some effects of micro-structure on reconstructed bone remodelling, Comptes Rendus Mécanique 340 (2012) 575–589.

Please cite this document as: A. Cazzani, M. Malagú, and E. Turco "Isogeometric analysis of plane–curved beams" *Mathematics and Mechanics of Solids*, 2016, 21(5): 562–577 DOI:10.1177/1081286514531265